Boletín de Geología
Vol. 27, No. 2, julio-diciembre de 2005

CATION SUBSTITUTIONS GOVERNING THE CHEMISTRY OF AMPHIBOLE IN THE SILGARÁ FORMATION METABASITES AT THE SOUTHWESTERN SANTANDER MASSIF

Ríos, C.A.[1]

ABSTRACT

Amphibole-bearing parageneses from the Silgará Formation metabasites at the southwestern Santander Massif record evidence of prograding metamorphism. Optical and microprobe analyses, together with thermobarometric estimates on these rocks, show that the main variation in Ca-amphibole is the simultaneous substitution of Al into the T1 site (Al^{IV}) and Na+K into the A-site of the amphibole's crystal structure. Al^{IV} is strongly temperature dependant, and this dependancy masks any pressure effect. Changes in the chemical composition of Ca-amphibole grains are interpreted through coupled substitutions, and reactions with co-existing minerals during an increase in metamorphic conditions from greenschist to lower amphibolite facies, being favourable circumstances record not only the metamorphic facies reached by rocks but also the P-T conditions by which these were attained.

Keywords: amphibole, Silgará, metabasites, substitution, metamorphic conditions

SUSTITUCIONES CATIÓNICAS QUE GOBIERNAN LA QUÍMICA DEL ANFÍBOL EN METABASITAS DE LA FORMACIÓN SILGARÁ EN LA REGIÓN SUROCCIDENTAL DEL MACIZO DE SANTANDER

RESUMEN

Las paragénesis con presencia de anfíbol de las rocas metabásicas de la Formación Silgará en la región suroccidental del Macizo de Santander registran evidencia de metamorfismo prógrado. Análisis ópticos y de microsonda electrónica, junto con cálculos termobarométricos en estas rocas, muestran que la principal variación en anfíboles cálcicos es la sustitución simultánea de Al en el sitio T1 (Al^{IV}) y Na+K en el sitio A de la estructura cristalina del anfíbol. Al^{IV} es fuertemente dependiente de la temperatura, y esta dependencia enmascara cualquier efecto de la presión. Los cambios en la composicion química del anfíbol cálcico son interpretados a traves de sustituciones acopladas, y reacciones con los minerales con los cuales coexiste durante un aumento en las condiciones de metamorfismo desde la facies esquisto verde hasta la facies anfibolita inferior, siendo circunstancias favorables que registran no solo las facies metamórficas alcanzadas por las rocas sino tambien las condiciones de P-T por las cuales estas fueron obtenidas.

Palabras claves: anfíbol, Silgará, metabasitas, sustitución, condiciones de metamorfismo

[1]Escuela de Geología, Facultad de Ingenierías Fisicoquímicas, Universidad Industrial de Santander, A.A 678, Bucaramanga, Colombia
e-mail: carios@uis.edu.co

INTRODUCTION

Amphibole-bearing metabasites are common in the Silgará Formation (SF) metamorphic sequence at the southwestern Santander Massif, and its chemistry document changes in P-T conditions. In order to gain a solid understanding of the metamorphism of these rocks under widely varying P-T conditions, it is very important to know the amphibole compositional variability, and the potential exchange mechanisms operating under different P-T regimes.

Metabasites of the SF in the greenschist and lower amphibolite facies often contain plagioclase (An_{1-51}), biotite, epidote, chlorite and quartz, along with amphibole, and a water rich fluid phase is likely to have accompanied the solid phases during metamorphism. Ríos (1999) analyzed the amphibole occurring in these rocks and found it to be calcic amphibole, which ranges in composition from tschermakite to magnesio-hornblende.
The significance of Ca-amphibole occurrence in the SF metabasites as indicator of changes in pressure and temperature is being pointed in this study. Numerous studies deal with Ca-amphiboles in metabasites (e.g., Leake, 1965; Raase 1974; Laird & Albee, 1981; Thompson *et al.*, 1982; Hawthorne 1983; Gilbert *et al.*, 1981; Robinson *et al.*, 1982; Moody *et al.*, 1983; Deer *et al.*, 1983; Graham & Powell, 1984; Kawakatsu & Yamaguchi, 1987; Blundy & Holland, 1990; Holland & Blundy, 1994; Anderson & Smith, 1995; Ernst & Liu, 1998), and make it clear that with increasing metamorphic grade, Ca-amphiboles exhibit increases in Mg/(Mg+Fe), and Ti, Al, Na, and K contents and decreases in Si content and total Fe+Mg+Mn±Ca.

These changes reflect increases in the tschermakitic, pargasitic and edenitic substitutions as a consequence of net-transfer reactions as well as exchange equilibria. However, it is very complex to relate Ca-amphibole chemistry to the conditions of metamorphism due to its crystal structure includes several cation sites capable of accommodating elements having a wide range of ionic radii and valences.

In this paper, I described not only the occurrence of Ca-amphibole and other associated mineral phases in the SF metabasites, but also show how a set of chemical reactions may control the chemistry of Ca-amphibole and that the variety of substitutions in this mineral can be favourable to consider this mineral as petrologic indicator not only of metamorphic facies but also of P-T conditions. Metabasites of the SF were studied in detail, using mineral chemistry, phase relationships and geothermobarometry, because they contain mineral assemblages appropriate for determining the metamorphic P-T conditions, which can be compared with those of metapelitic rocks.

GEOLOGICAL SETTING

The Lower Paleozoic Silgará Formation, which forms part of the pre-Devonian basement exposed at the southwestern Santander Massif, is a metamorphic sequence of low to middle grade that consists of metapelitic rocks with interbedded metabasites intruded by granitoids (FIGURE 1). This metamorphic unit displays a well developed schistosity, although locally shows well-preserved bedding (cross lamination). The lithology of the pelitic sequence changes in composition southwestward, from psammitic schists more feldspathic at Pescadero through semipelitic schists to pelitic schists more quartz-rich rocks at the Mesa de San Pedro.

The regional geology of the study area has been summarized based on earlier work by Ward *et al.* (1973). The metamorphic sequence of the SF generally strikes NW-SE and dips to the southwest, but it is very folded. On the southwest, the SF is very faulted (e.g., Los Santos - Aratoca Fault) and is discordantly overlain by Mesozoic sedimentary rocks. On the northeast, it underlains the Mesozoic volcanic and sedimentary rocks at the Mesa de Los Santos. In the study area, the SF is cut by intrusive bodies of Triassic-Jurassic age (193±6 Ma; K-Ar age, Goldsmith et al., 1971), which forms part of the Santander Plutonic Complex, and are interpreted as calc-alkaline crustal bodies emplaced after peak-metamorphism. The age of this magmatism was latter supported by Dörr et al. (1995) and Ordoñez (2003). The igneous bodies of the Santander Plutonic Complex intrude not only into the Middle Devonian and/ or younger sediments but also into the pre-Devonian metamorphic rocks and they are overlain by Middle Devonian sedimentary rocks indicating their pre-Devonian age. The low-grade Floresta Formation, which overlain discordantly the SF, contains fossil evidence that indicates Middle Devonian age (Forero, 1990). Therefore, this metamorphic unit is clearly pre-Middle Devonian. Regional metamorphism, uplift and erosion may have occurred between the accumulation of the protholith of the SF and the accumulation of the Floresta Formation. Different studies on metamorphism have been developed at the southwestern Santander Massif (e.g., Castellanos, 1999; García & Castellanos, 1998; Schäfer *et al.*, 1998; Ríos, 1999, 2001; Ríos & Takasu, 1999; García & Ríos, 1999; Ríos, 2001; Ríos & García, 2001; Mantilla *et al.*,

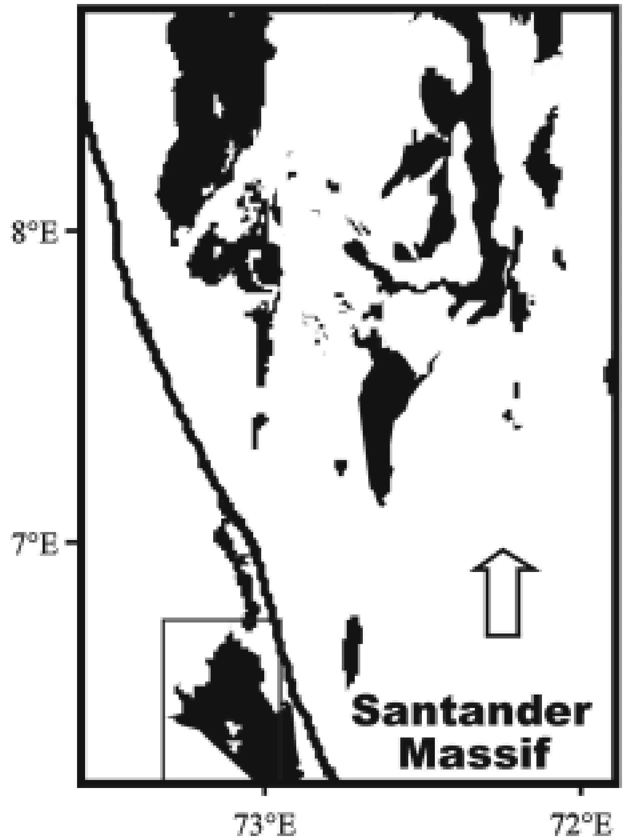

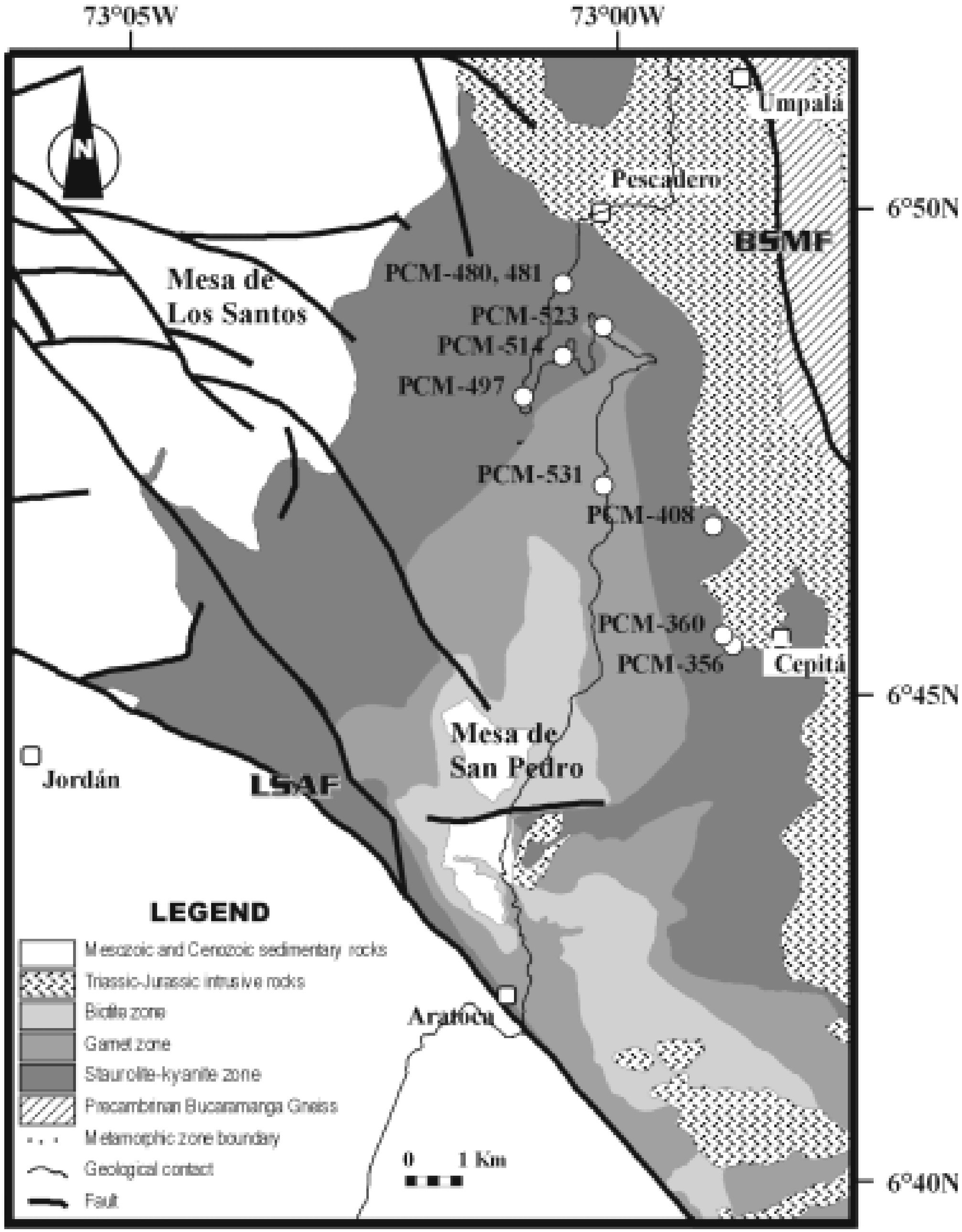

FIGURE 1. Distribution of the Silgará Formation metamorphic rocks at the Santander Massif (modified after Goldsmith et al., 1971), on left side. Generalized geological map of the southwestern Santander Massif (modified after Ward et al., 1973), on right side, the sample localities are indicated by white dots. In grey scale are shown the metamorphic zones of the Silgará Formation. BSMF: Bucaramanga – Santa Marta Fault; LSAF: Los Santos – Aratoca Fault.

2001, 2002; Gélvez & Márquez, 2002; Ríos *et al.*, 2003; Mantilla *et al.*, 2003). Ríos (1999) carried out a detail study about the chemical composition of the constituent minerals of the SF metamorphic rocks and the P-T conditions of metamorphism. Schäfer *et al.* (1998) reported for the first time the occurrence of metabasites within the pre-Devonian Silgará Formation, developing a study of their metamorphism and geochemistry, and establishing a magmatic origin for these rocks.

The rocks of interest in this study are referred as the metabasites (e.g., amphibole-bearing schists, orthoamphibolites, and garnet-bearing metabasites) of the SF. They are too small to be distinguished separately at the map scale, and they may represent dykes and sills emplaced prior to deformation and metamorphism. This study attempts to elucidate the metamorphic parageneses of the SF metabasites, as well as establish the role of chemical reactions may control the chemistry of Ca-amphibole as a petrologic indicator of P-T conditions, and therefore to make further constraints on the P-T history of this metamorphic sequence at the southwestern Santander Massif.

PETROGRAPHY OF METABASITES

In FIGURE 2 is illustrated the main petrographical features from metabasites of the SF in the study area. Detailed petrographic study of thin sections was carried out on 9 specimens. Mineral abbreviations are after Kretz (1983). These rocks comprise well-foliated amphibole-bearing schists, orthoamphibolites and garnet-bearing metabasites, which contain medium-grained nematoblasts of idioblastic hornblende, and most of the rocks have a schistosity defined by a preferred orientation of hornblende, biotite and epidote. The main fabric is sometimes overgrown by post-tectonic amphibole porphyroblasts (FIGURE 2c). Plagioclase and quartz form a fine-grained, granoblastic matrix, with local plagioclase porphyroblasts in augen structure (FIGURE 2d). These rocks are mainly compossed by amphibole, biotite, plagioclase, quartz, epidote, with accesory minerals such as sphene, apatite, zircon, Fe-Ti oxides and calcite.

Ca-amphibole occurs as prismatic crystals, usually elongate, which show an idioblastic to subidioblastic character (from 0.15x0.05mm to 1x0.2mm in longitudinal section, and from 0.25x0.08mm to 1x0.2mm in cross section). It shows pleochroism x’: yellow-green and z’: green, and simple lamellar twinning. It has a preferred orientation, developing the schistosity with coexisting biotite and epidote. Calcic amphibole overgrows the S_1 fabric, developing cross foliations, and also occurs as randomly oriented, large, poikiloblastic and post-tectonic porphyroblasts, which have overgrown the main schistosity and contain inclusions of quartz, plagioclase and ilmenite (FIGURE 2c). Pseudomorphs of chlorite after calcic amphibole occur (FIGURE 2e), but it is usually partly replaced by chlorite or biotite, and in garnet-bearing metabasites it is partially replaced by chlorite, epidote and calcite.

Plagioclase shows a subidioblastic to xenoblastic character (0.1x0.06mm, average, up to 0.25x0.08mm in size), and occurs as a matrix phase associated with quartz (FIGURE 2a, 2b, 2d, 2e) or as augen, developing poikiloblasts (0.2x0.1mm, average, up to 1.75x1.5mm), which includes quartz, biotite, amphibole, epidote, and apatite (FIGURE 2d). It usually does not show twinning in the matrix, but porphyroblasts always show albite multiple twinning. Plagioclase is breaking down to sericite.

Biotite is brown and strongly pleochroic (x: yellow, y: brown, and z: brown), and shows a subidioblastic character. It occurs as flaky crystals (0.15mmx0.02mm in size, average) that displays straight and serrated boundaries and develops a directional nematolepidoblastic fabric along with amphibole and epidote (FIGURE 2c). Biotite is breaking down to chlorite, and it also sometimes occurs along the cracks of amphibole as a retrograde phase.

Garnet-bearing metabasites show a variably developed schistosity, S_2 (FIGURE 2a, 2b) and lineation related to D_2 deformation. Garnet occurs as numerous fine- to medium-grained crystals (0.1-3.3 mm diameter, average) with an anhedral to subhedral and pseudohexagonal and rounded shape. It contains abundant quartz inclusions in core regions, and other inclusions are epidote, plagioclase, biotite, and ilmenite, the last of them locally aligned parallel to the main foliation of the rock.

Epidote occurs in aggregates of elongate prismatic crystals (subidioblastic to xenoblastic character) with 0.05mmx0.025mm, average, up to 0.3mmx0.05mm in size, is colourless to pale yellownish green, showing slight pleochroism (x: colourless to pale yellownish green, y: greenish and z: yellownish, moderate to high birefringence and optical zoning (FIGURE 2f). It also occurs after amphibole as a retrograde phase.

Quartz shows a xenoblastic character and rounded shape (0.1x0.05mm, average, up to 0.25x0.15mm), commonly

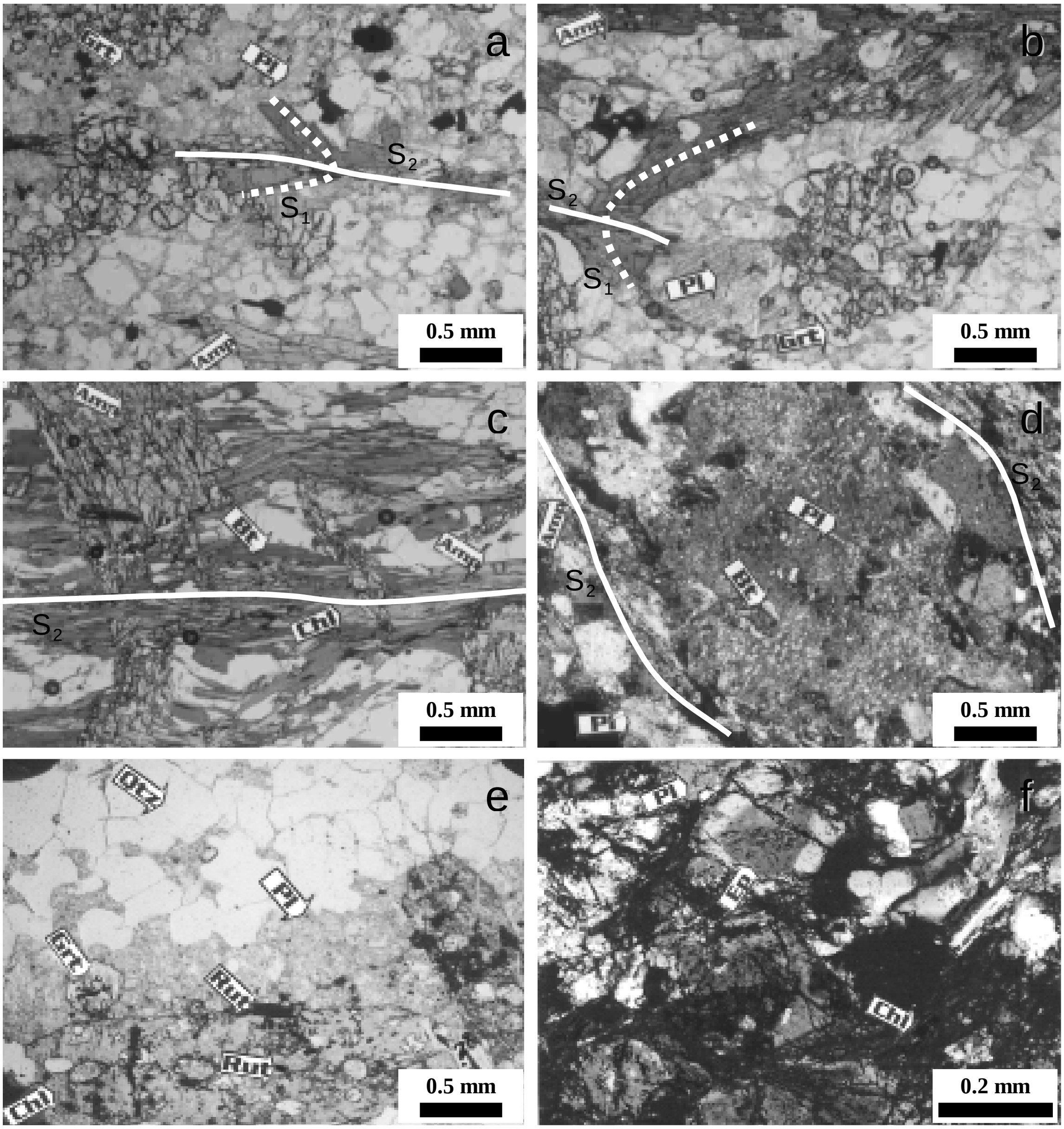

FIGURE 2. Petrographic features from metabasites of the Silgará Formation at the southwestern Santander Massif. (a) Small garnet neoblasts associated to Ca-amphibole and opaque minerals in a garnet-bearing metabasite (PCM-514). Ca-amphibole develops two schistosity surfaces. Plane-polarized light. (b) Large and idioblastic garnet porphyroblast, which consists of inclusion-rich core and inclusion-free rim, is associated to Ca-amphibole in a garnet-bearing metabasite (PCM-514). Plane-polarized light. (c) Ca-amphibole porphyroblasts overgrow the main schistosity in a basic schist (PCM-497), and contain inclusions of quartz and ilmenite which develop a S_{int} parallel to S_{ext}. Plane-polarized light. (d) Ca-amphibole developing the main foliation along with biotite and epidote of a basic schist (PCM-356), which wraps augen plagioclase that shows incipient alteration to sericite, but still displays multiple twinning. Cross-polarized light. (e) Chlorite pseudomorph after Ca-amphibole porphyroblasts, which still retain its original shape, in a garnet-bearing metabasite (PCM-523). Plane-polarized light. (f) Epidote, displaying optical zoning, associated to chlorite in a basic schist (PCM-408). Cross-polarized light.

developing granular aggregates with plagioclase (FIGURE 2e), and around plagioclase porphyroblasts in augen structure, which is wrapped by nematolepidoblastic bands of hornblende, biotite and epidote. It shows a wavy extinction and rounded boundaries with plagioclase and straight boundaries when is bounded by biotite and/or amphibole.

Sphene shows an idioblastic to subidioblastic character, often occuring as small diamond-shaped crystals

(0.05mmx0.025mm, average, up to 0.15mmx0.05mm), and is pale brown or dark brown. Apatite occurs as colourless, low-birefringent, near-isotropic, high relief, and subidioblastic to xenoblastic crystals (0.08mmx0.04mm, average, up to 0.25mmx0.1mm) in the groundmass or as idioblastic inclusions in plagioclase. Zircon shows a xenoblastic character (0.03mmx0.015mm, average, up to 0.1mmx0.025mm), high relief, high birefringence, and occurs in the groundmass.

Chlorite shows a pale green color, pleochroism (x: pale green to colourless, y: darker green, and z: darker green), and anomalous interference colours (light gray and anomalous brown). It occurs as a retrograde phase after biotite or amphibole along the cleavage of these minerals or after amphibole as pseudomorh, which preserves the original shape of the amphibole.

Calcite locally occurs developing lenses concordant to the main schistosity of the rock inside of the nematolepidoblastic fabric.

METAMORPHISM

The stability ranges of minerals and mineral assemblages of the SF metabasites are shown in TABLE 1. The typical mineral assemblages in these rocks are Mg-Hbl (or Ts) ± Bt + Pl (+Qtz) and Ep + Bt + Mg-Hbl (or Ts) + Pl.

TABLE 1. Progressive mineral changes with metamorphism from metabasites of the Silgará Formation in the southwestern Santander Massif. Black bars: constituent minerals, and grey bars: accesory phases (sphene, ilmenite and rutile).

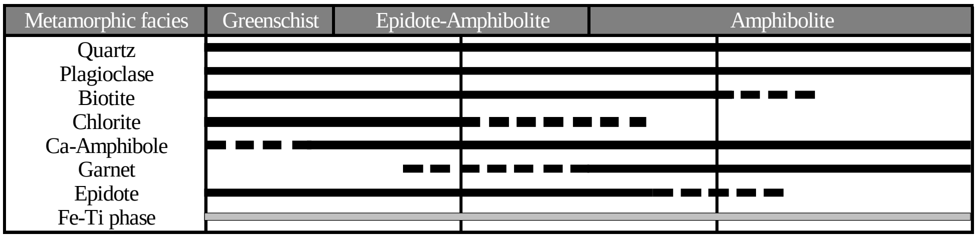

Garnet-bearing matabasites contain the assemblage Grt + Ts + Qtz + Pl. Accessory minerals are apatite, zircon, calcite, and Fe-Ti oxides.

The mineral assemblages in these rocks indicate that they have been equilibrated under metamorphic conditions from the greenschist facies to the lower amphibolite facies. The SF reached the lower amphibolite facies as the peak of metamorphism and then was affected by a retrograde metamorphism may be into the epidote-amphibolite facies (Ríos, 1999). Retrogressive effects are stronger in rocks near to the contact with the intrusive bodies. Metabasites of the SF show evidence of retrograde metamorphism, and many of the retrograde mineral changes involve hydration processes. Retrograde reactions include partial replacement of biotite by chlorite, amphibole by biotite and/or chlorite and plagioclase by sericite. Additional evidence of retrograde metamorphism is observed in biotite that shows ilmenite exsolution. Needle-shaped crystals of ilmenite occur in the three directions within biotite. It is known that the quantity of Ti component of biotite increases with increasing metamorphic grade. Therefore, ilmenite may form out of the excess quantity of Ti expelled from biotite during retrograde metamorphism.

ANALYTICAL PROCEDURE

Electron microprobe analyses were performed on the constituent minerals from 9 samples, using a JEOL JXA 8800M electron microprobe analyzer of the Department of Geosciences at Shimane University, under the following analytical conditions: accelerating voltage and specimen current are 15 kV and $2.0x10^{-8}$ Å, respectively. Data acquisition and reduction were performed using the correction method of Bence & Albee (1968). Natural and synthetic minerals were used as standards. Mineral compositions were determined by multiple spot analyses. The Ca-amphibole formulae were calculated on an anhydrous basis to a total of 13 cations, excluding Ca, Na and K, per 23 atoms of oxygen, using the charge-balance method to assign ferrous and ferric iron, and the cations assigned to each site according to IMA guidelines (Leake et al., 1997).

Amphibole chemistry

According to Leake et al. (1997), the classification of the amphiboles is based on the chemical contents of the standard amphibole formula represented by $AB_2C^{VI}_5T^{IV}_8O_{22}(OH)_2$, and the components of this formula conventionally described as A, B, C, T and "OH" correspond to the following crystallographic sites: A (1 site per formula unit); B (2 M4 sites per formula unit); C (a composite of 5 sites made up of 2M1, 2M2 and 1M3 sites per formula unit); T (8 sites, in two sets of 4, per formula unit, which need not be distinguished here); "OH" (2 sites per formula unit).

As shown in TABLE 2, the ions considered normally to occupy these sites are in the following categories:

Leake et al. (1997) suggest that the standard amphibole formula should be calculated, taking into account the following aspects:

TABLE 2. Ions considered normally to occupy the A, B, C, T and "OH" sites of the amphibole (after Leake et al., 1997).

Ions	Sites
□ (empty site) and K	A
Na	A or B
Ca	B
L type ions (Mg, Fe^{2+}, Mn^{2+}, Li, and rare ions of similar size such as Zn, Ni, Co)	C or B
M type ions Al	C or T
Fe^{3+} and more rarely Mn^{3+}, Cr^{3+}	C
High valence ions Ti^{4+}	C or T
Zr^{4+}	C
Si	T
Anions (OH, F, Cl, O)	"OH"

(1) If H_2O and halogen contents are well established, the formula should be calculated to 24(O,OH,F,Cl).
(2) If those are uncertain, on the basis of 23(O) with 2(OH,F,Cl), appropriate change in the assumed number of (OH+F+Cl) should be made.
(3) SumT = 8.00 using Si, then Al, then Ti. Fe^{3+} is not allocated to T for simplicity.
(4) SumC = 5.00 using excess Al and Ti from (3) and then successively Zr, Cr^{3+}, Fe^{3+}, Mn^{3+}, Mg, Fe^{2+}, Mn^{2+} and other L^{2+} type ions, and then Li.
(5) SumB = 2.00 using excess Mg, Fe^{2+}, Mn^{2+} and Li from (4), then Ca, and then Na.
(6) Excess Na from (5) is assigned to A, then all K. SumA = 0.00-1.00.

Representative mineral compositions of amphibole from metabasites of the SF are given in TABLE 3. Amphibole corresponds to calcic amphibole defined as monoclinic amphibole in which Ca_B³1.50, $(Na+K)_A<0.50$, and $Ca_A<1.50$, according to the terminology of Leake et al. (1997), and ranges in composition from tschermakite to magnesio-hornblende (FIGURE 3). The number of Si in tetrahedral sites (based on 23 oxygens) ranges from 6.099 to 7.487. The Mg/(Mg+Fe^{2+}) ratio ranges from 0.50 to 0.91. Al^{IV} and Al^{VI} in Ca-amphibole ranges from 0.513 to 1.901 and 0.120-0.958, respectively.

Holland & Blundy (1990) discussed amphibole chemistry in terms of several endmember compositions related, by simple coupled substitutions, to a compositionally simple endmember such as tremolite. Coupled substitution comprises the simultaneous introduction of cations (or anions) into two or more amphibole sites in the proportions required maintaining charge balance. The most common amphibole substitutions are given in TABLE 4.

Chemistry of associated phases

Microprobe analyses of phases coexisting with Ca-amphibole in metabasites of the SF are listed in TABLE 5. In FIGURE 4 is shown a back-scattered electron image of the Ca distribution within associated mineral phases (Ca-amphibole, garnet and plagioclase) in a garnet-bearing metabasite (PCM-514) from the staurolite-kyanite zone. Garnet in this metabasite contains the highest proportion of CaO of all analyzed garnet-bearing samples from the SF metamorphic sequence studied by Ríos (1999), who reports strong irregularities and fluctuations in the distribution of Ca in garnet that displays oscillatory zoning, which can be likely related to reactions involving garnet and other calcic phases in this rock (hornblende, plagioclase, epidote). Plagioclase also shows an oscillatory zoning in Ca content, with the lowest value near rim. However, Ca-amphibole shows a homogenous distribution of Ca content.

Biotite. Al^{IV} varies from 1.921 to 2.910, and Al^{VI} varies from 0.332 to 1.666, indicating slight solid solution towards the dioctahedral micas, and Al and Ti contents of biotite are 2.253-4.576 and 0.005-0.272 per formula unit (pfu), respectively. Biotite compositions are plotted on part of the phlogopite-annite-eastonite-siderophyllite quadrilateral. The Fe/(Fe+Mg) ratios of biotite range from 0.29 to 0.38.

TABLE 3. Representative chemical compositions of Ca-amphibole from metabasites of the Silgará Formation at the soutwestern Santander Massif.

Lithology	GBM	GBM	GBM	GBM	A	A	A	MS	MS	MS	MS	A	A	MS	MS	MS
Met. Zone	St-Ky	St-Ky	St-Ky	St-Ky	Grt	Grt	Grt	St-Ky	St-Ky	St-Ky	St-Ky	St-Ky	St-Ky	St-Ky	St-Ky	St-Ky
Sample	PCM-514	PCM-514	PCM-514	PCM-514	PCM-531	PCM-531	PCM-531	PCM-356	PCM-356	PCM-481	PCM-481	PCM-497	PCM-497	PCM-480	PCM-480	PCM-480
Analysis	120	125	154	158	51	84	88	94	97	10	12	51	54	1	82	83
Weight %	mat.	inc.	core	rim	inc.	core	rim	rim	core	rim	core	rim	core	inc.	core	rim
SiO_2	41,06	40,25	41,40	40,97	45,72	43,31	49,73	45,61	44,46	47,48	47,73	45,61	44,75	45,38	46,61	45,84
TiO_2	0,42	0,77	0,41	0,40	0,30	0,26	0,15	0,42	0,41	0,42	0,38	0,35	0,35	0,50	0,50	0,52
Al_2O_3	15,23	15,09	15,03	15,13	11,28	13,00	5,27	9,83	10,77	9,23	8,81	12,79	13,54	11,06	10,31	10,50
FeO *	16,62	18,01	16,61	16,69	13,37	16,04	17,71	13,37	13,34	11,92	11,51	11,49	13,74	13,79	13,37	14,01
MnO	0,63	0,56	0,63	0,69	0,30	0,12	0,29	0,32	0,26	0,23	0,31	0,49	0,41	0,37	0,35	0,36
MgO	8,31	7,46	8,60	8,32	13,48	11,30	12,01	13,28	13,07	13,89	14,13	13,57	12,00	12,39	13,06	12,81
CaO	11,15	11,17	11,02	11,00	11,72	11,73	12,10	12,57	12,44	12,68	12,92	12,34	11,97	12,72	12,70	12,66
Na_2O	1,66	1,53	1,67	1,61	1,80	1,77	0,66	1,29	1,27	0,97	0,95	1,27	1,56	1,21	1,10	1,35
K_2O	0,35	0,34	0,30	0,30	0,19	0,31	0,19	0,41	0,55	0,67	0,64	0,25	0,27	0,89	0,77	0,75
Cr_2O_3	0,01	0,02	0,02	0,01	0,01	0,06	0,00	0,25	0,33	0,16	0,13	0,06	0,18	0,06	0,05	0,06
Total	95,44	95,20	95,69	95,12	98,17	97,90	98,11	97,35	96,90	97,65	97,51	98,22	98,77	98,37	98,82	98,86
Cations per 23 oxygens																
Si	6,196	6,137	6,210	6,190	6,548	6,313	7,263	6,680	6,544	6,893	6,944	6,502	6,414	6,621	6,726	6,642
Ti	0,048	0,088	0,046	0,045	0,032	0,028	0,016	0,046	0,045	0,046	0,042	0,037	0,038	0,055	0,054	0,057
Al	2,709	2,711	2,657	2,694	1,904	2,233	0,907	1,697	1,868	1,579	1,511	2,149	2,287	1,902	1,753	1,793
Fe 3+	0,641	0,665	0,738	0,742	0,801	0,842	0,526	0,376	0,449	0,146	0,058	0,588	0,589	0,243	0,292	0,342
Fe 2+	1,495	1,665	1,379	1,401	0,828	1,149	1,662	1,275	1,209	1,306	1,344	0,799	1,079	1,449	1,332	1,369
Mn	0,080	0,072	0,080	0,088	0,036	0,015	0,036	0,040	0,032	0,028	0,038	0,059	0,050	0,046	0,043	0,044
Mg	1,870	1,696	1,923	1,874	2,878	2,456	2,615	2,900	2,868	3,006	3,065	2,884	2,564	2,695	2,810	2,767
Ca	1,803	1,824	1,771	1,780	1,798	1,832	1,893	1,972	1,962	1,972	2,014	1,884	1,838	1,988	1,963	1,965
Na	0,486	0,452	0,486	0,472	0,500	0,500	0,187	0,366	0,362	0,273	0,268	0,351	0,433	0,342	0,308	0,379
K	0,067	0,066	0,057	0,058	0,035	0,058	0,035	0,077	0,103	0,124	0,119	0,045	0,049	0,166	0,142	0,139
Cr	0,001	0,002	0,002	0,001	0,001	0,007	0,000	0,029	0,038	0,018	0,015	0,007	0,020	0,007	0,006	0,007
Total	15,387	15,379	15,350	15,346	15,362	15,433	15,140	15,458	15,482	15,392	15,417	15,305	15,363	15,512	15,429	15,503
Si	6,196	6,137	6,210	6,190	6,548	6,313	7,263	6,680	6,544	6,893	6,944	6,502	6,414	6,621	6,726	6,642
Al^{IV}	1,804	1,863	1,790	1,810	1,452	1,687	0,737	1,320	1,456	1,107	1,056	1,498	1,586	1,379	1,274	1,358
sum T	8,000	8,000	8,000	8,000	8,000	8,000	8,000	8,000	8,000	8,000	8,000	8,000	8,000	8,000	8,000	8,000
Al_{VI}	0,905	0,848	0,867	0,884	0,452	0,546	0,170	0,377	0,412	0,473	0,455	0,650	0,701	0,522	0,480	0,435
Ti	0,048	0,088	0,046	0,045	0,032	0,028	0,016	0,046	0,045	0,046	0,042	0,037	0,038	0,055	0,054	0,057
Fe 3+	0,641	0,665	0,738	0,742	0,801	0,842	0,526	0,376	0,449	0,146	0,058	0,588	0,589	0,243	0,292	0,342
Cr	0,001	0,002	0,002	0,001	0,001	0,007	0,000	0,029	0,038	0,018	0,015	0,007	0,020	0,007	0,006	0,007
Mg	1,870	1,696	1,923	1,874	2,878	2,456	2,615	2,900	2,868	3,006	3,065	2,884	2,564	2,695	2,810	2,767
Fe 2+	1,495	1,665	1,379	1,401	0,828	1,121	1,662	1,272	1,187	1,306	1,344	0,799	1,079	1,449	1,332	1,369
Mn	0,050	0,036	0,044	0,053	0,007	0,000	0,011	0,000	0,000	0,005	0,022	0,035	0,008	0,030	0,027	0,025
sum C	5,000	5,000	5,000	5,000	5,000	5,000	5,000	5,000	5,000	5,000	5,000	5,000	5,000	5,000	5,000	5,000
Mg	0,000	0,000	0,000	0,000	0,000	0,000	0,000	0,000	0,000	0,000	0,000	0,000	0,000	0,000	0,000	0,000
Fe 2+	0,000	0,000	0,000	0,000	0,000	0,029	0,000	0,003	0,022	0,000	0,000	0,000	0,000	0,000	0,000	0,000
Mn	0,031	0,036	0,036	0,036	0,029	0,015	0,025	0,040	0,032	0,023	0,017	0,025	0,042	0,016	0,016	0,020
Ca	1,803	1,824	1,771	1,780	1,798	1,832	1,893	1,972	1,962	1,972	2,014	1,884	1,838	1,988	1,963	1,965
$Na_{(B)}$	0,166	0,139	0,193	0,184	0,172	0,125	0,082	0,000	0,000	0,005	0,000	0,091	0,120	0,000	0,020	0,015
sum B	2,000	2,000	2,000	2,000	2,000	2,000	2,000	2,015	2,016	2,000	2,031	2,000	2,000	2,004	2,000	2,000
$Na_{(A)}$	0,319	0,313	0,293	0,288	0,327	0,375	0,105	0,366	0,362	0,268	0,268	0,260	0,313	0,342	0,287	0,364
K	0,067	0,066	0,057	0,058	0,035	0,058	0,035	0,077	0,103	0,124	0,119	0,045	0,049	0,166	0,142	0,139
sum A	0,387	0,379	0,350	0,346	0,362	0,433	0,141	0,443	0,466	0,392	0,387	0,305	0,363	0,508	0,429	0,503
Total	15,387	15,379	15,350	15,345	15,362	15,433	15,140	15,458	15,482	15,392	15,417	15,305	15,363	15,512	15,429	15,503
X_{Mg}	0,557	0,505	0,582	0,572	0,776	0,681	0,611	0,695	0,703	0,697	0,695	0,783	0,704	0,650	0,678	0,669

***Total Fe as $FeO+Fe_2O_3$. Fe^{3+} from stoichiometry according to Leake et al. (1997). $X_{Mg} = Mg/(Mg+Fe^{2+})$.**
Abreviations: MS (mafic schist), A (amphibolite), GBM (garnet-bearing matabasite), mat. (matrix), inc. (inclusion).

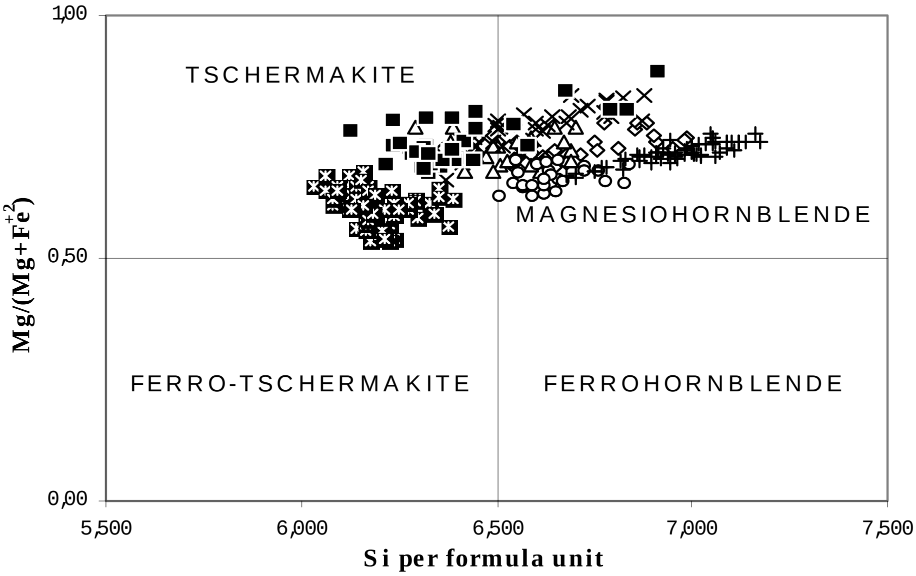

FIGURE 3. Ca-amphibole compositions (based on 23 oxygens per formula unit, pfu) from metabasites of the SF, according to Leake et al. (1997). Diagram parameters: $Ca_B \geq 1.50$; $(Na+K)_A < 0.50$; $Ca_A < 0.50$.

The change in composition from biotite to phlogopite is probably controlled by the bulk-rock chemistry.

Plagioclase. The anorthite content of plagioclase, expressed as X_{An}, in metabasic rocks ranges from 0.01 to 0.51, showing a peristerite gap between An_5 and An_{14}. The maximum anorthite content in plagioclase reflects the higher temperature condition during prograde metamorphism. The zoning patterns often show that matrix plagioclase typically displays reversal zoning according to the X_{An} from core to rim. The increase in An content of plagioclase rims is related to plagioclase rims in contact with Ca-amphibole or near apatite. The orthoclase content in plagioclase is $Or_{0.11-5.98}$.

Garnet. It occurs in garnet-bearing metabasites (e.g., sample PCM-514), in which garnet is richer in grossular content (X_{grs}= 0.17-0.24) than that in those free in Ca-amphibole (X_{grs}= 0.02-0.19), suggesting that the first of them reflect more Ca-rich bulk compositions than do the last of them. The grossular component displays oscillatory zoning, fluctuating between 17 and 24 mol%. From core to rim, spessartine decreases and Fe/(Fe+Mg) increases, and there are two peaks in grossular concentrations. The variable grossular content is likely related to reactions involving other calcic phases in this rock (hornblende, plagioclase, epidote).

Epidote mineral group. Epidote shows minor amounts of Mn (0.000-0.166). The $Fe^{2+}/(Fe^{2+}+Al)$ ratio ranges from 0.11 to 0.36. It shows commonly optical zoning, but its chemical zoning patterns often show inconsistent relationships.

Fe-Ti oxides. Accesory titanite, ilmenite, and rutile are Ti-rich phases coexisting with the silicates. Representative mineral compositions of Fe-Ti oxides are given in TABLE 3. According to Neogi *et al.* (1997), rutile is stable at higher P (P > 1.6Gpa at T³ 800°C, and P > 1.4Gpa at T = 700°C), ilmenite is stable at lower P and high T (P < 1.6Gpa at T³ 800°C), and titanite is stable at relatively low P and low T (P > 1.4Gpa at T = 700°C).

Chlorite. According to the classification proposed by Hey (1954), chlorite mainly corresponds to ripidolite, partly to pycnochlorite and, in lesser extent to brunsvingite. X_{Mg} of chlorite ranges from 0.27-0.75. All chlorites contain small, but consistent, amounts of Mn, which ranges from 0.002 to 0.331 a.p.f.u. Samples are pycnochlorite-brunsvigite-ripidolite solid solutions with 4.963-6.229 Si, and, in general, carry approximately equal amounts of Al^{IV} and Al^{VI}.

GEOTHERMOBAROMETRY

In well-equilibrated mineral assemblages, particularly those cooled rapidly and not subject to retrogression, quantitative P-T estimates may be obtained from geothermobarometry. P-T conditions were estimated for metabasites of the SF, using the rim composition of amphibole and plagioclase. Garnet in garnet-bearing metabasites shows a moderate to strong chemical zoning, and the rim composition of

TABLE 4. Summary of amphibole end member compositions and their substitutions relative to tremolite site allocation details for amphiboles based on Hawthorne (1983). General formula: $A(M4)_2(M13)_3(M2)_2(T2)_4(T1)4O_{22}(O,OH,F)_2$. The symbol Ž denotes vacancy.

Symbol		A	M4	M13	M2	T2	T1
Tremolite			Ca_2	Mg_3	Mg_2	Si_4	Si_4
Edenite		Na	Ca_2	Mg_3	Mg_2	Si_4	$AlSi_3$
Hornblende			Ca_2	Mg_3	MgAl	Si_4	$AlSi_3$
Pargasite		Na	Ca_2	Mg_3	MgAl	Si_4	Al_2Si_2
Site allocations:							
T2		Si					
T1		Si, Al^{IV}					
M2		Al^{VI}, Fe^{3+}, Ti, Cr, (Mg, Fe^{2+})					
M13		Mg, Fe^{2+}, (Mn)					
M4		Ca, Na, Mn, (Fe^{2+}, Mg)					
A		K, Na, ?					

garnet was used to determine peak temperature and pressure conditions of metamorphism.

The coexisting mineral assemblage amphibole-plagioclase is an useful geothermometer. Spear (1980) considers that plagioclase and amphibole are non-ideal along the $NaSiCa_{-1}Al_{-1}$ vector and partitioning is highly dependent upon composition. Partitioning coefficients are moderately dependent on T and weakly dependent on P, although compositional effects tend to mask these dependencies. Blundy & Holland (1990) proposed a pressure-dependent geothermometer based on the tetrahedral aluminum content in calcic amphibole and the albite content in plagioclase, which should only be used between 500-1100°C and for assemblages with plagioclase less calcic than An_{92} and with amphiboles with less than 7.8 Si atoms pfu. However, the pressure dependence is poorly constrained and the equilibria are not suitable for barometry. This geothermometer has been discussed by different autors (Hammarstrom & Zen, 1992; Rutherford & Johnson, 1992; Poli & Schmidt, 1992), who consider that the geobarometer provided by the amphibole-plagioclase assemblage can be extremately useful when applied to quartz-saturated rocks. A recent calibration of the amphibole-plagioclase equilibrium is proposed by Holland & Blundy (1994). They present two modern calibrations of the previous version for edenite-tremolite and hornblende-plagioclase exchange vectors, which take into account non-ideal mixing in both amphibole and plagioclase and are calibrated against an extensive data set of natural and synthetic amphiboles. On the other hand, Graham & Powell (1984) provide a garnet-hornblende thermometer, which is applicable below about 850°C to rocks with Mn-poor garnet and common hornblende of widely varying chemistry metamorphosed at low a_{O2}. The amphibole-plagioclase thermometer of Spear (1980) was also used.

Metamorphic temperatures from amphibole-bearing rocks of the SF were estimated using edenite/richterite exchange reactions between amphibole and plagioclase (Spear, 1980; Holland & Blundy, 1994) and garnet-amphibole (Graham & Powell, 1984) geothermometers. The anlyzed samples are distributed throughout the study area and yield anomalous high temperatures of 753-996°C in metamafic

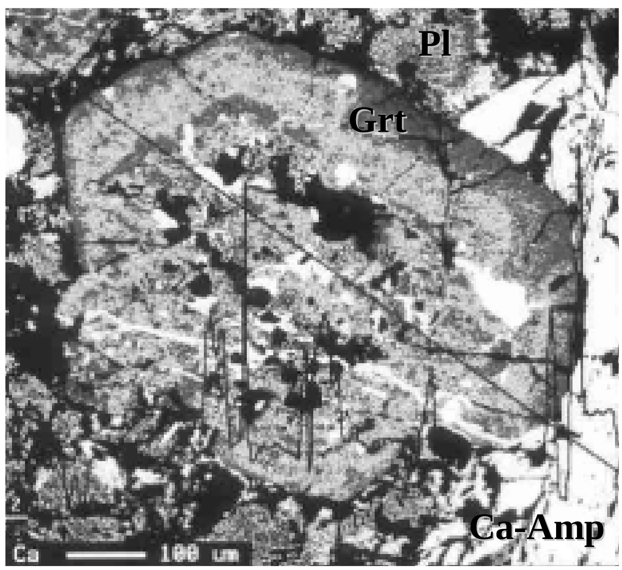

FIGURE 4. Back-scattered electron image showing the Ca distribution within associated mineral phases (Ca-amphibole, garnet and plagioclase) in a garnet-bearing metabasite (PCM-514) from the staurolite-kyanite zone. The white areas correspond to the highest Ca content and the black areas correspond to the lowest Ca content.

rocks, and 823-890^{o}C in garnet-bearing metabasites using the geothermometer of Holland & Blundy (1994). Using the garnet-hornblende thermometer of Graham & Powell (1984) in garnet-bearing metabasites temperature ranges between 507 and 551^{o}C, while using the amphibole-plagioclase thermometer of Spear (1980) temperatures are 587-597^{o}C and 376-527^{o}C in garnet-bearing metabasites and garnet-free metabasites, respectively. These results corroborate the temperatures obtained by Ríos (1999) from metapelitic rocks.

Barometry is problematic as different barometers applied to the same sample give a wide range in pressures. However, pressures were estimated using the aluminium-in-hornblende geobarometer of Johnson & Rutherford (1989) in metamafic rocks (4.4-5.6 kbar), and the garnet-amphibole-plagioclase-quartz geobarometer of Kohn & Spear (1989) in garnet-bearing metabasites (4.9-5.2 kbar). On the other hand, as shown in the $Na_{(B)}$ vs Al^{IV} diagram (FIGURE 5), analized Ca-amphibole are plotted, showing low $Na_{(B)}$ values, with variable Al^{IV} contents. Higher values of $Na_{(B)}$ corresponding to higher Al^{IV} contents, and belong to the shadow area of Sierra Nevada (USA), which characterize low pressure conditions (approximately 2.0 kbar).

DISCUSSION ON Ca-AMPHIBOLE AS A PETROGENETIC INDICATOR

The compositions of amphiboles can be used to delineate metamorphic grade and facies series, inamuch as the analyzed metabasites contain the common assemblage, Ca-amphibole + chlorite + epidote + plagioclase + quartz + Fe-Ti-phase.

FIGURE 6d shows how substitution of Al^{IV} for Si in tetrahedral sites is mainly coupled with the substitution of Al^{VI}, Fe^{3+}, Ti and $(Na+K)_A$ in octahedral sites. According to Kawakatsu & Yamaguchi (1987), A-site occupancy of Na and K should be balanced mainly by the residual tetrahedral charge and partly by substitution of Na for Ca in M4.

As shown in FIGURE 6a, Ca-amphibole from the metabasites of the SF are plotted mainly within the biotite and garnet zones, and in the boundary between the garnet and staurolite-kyanite zones according to Laird & Albee (1981). According to them, Ca-amphibole belongs to the greenschist and lower amphibolite facies series. These results are consistent with those found in metapelitic rocks. The principal variation in Ca-amphibole is the simultaneous substitution of Al into the T1 site (Al^{IV}) and Na+K into the A-site, as shown in FIGURE 6b. Al^{IV} is strongly temperature dependant, and this dependancy, which masks any pressure effect, and the evidence of Al^{IV}-$(Na+K)_A$ coupling indicates that the $(Na+K)_A$,Al^{IV} = **?**$_A$,Si exchange is mainly a function of temperature (Blundy & Holland, 1990). A geothermal trend may be drawn in the Al^{IV}-$(Na+K)_A$ diagram (FIGURE 6b), which has a purely prograde part, which pass near the tremolite-pargasite tie line. The Al^{IV}-Na_A-rich Ca-amphibole of each trend is characteristic of the peak of metamorphism. This figure shows that the predominant variation in calcic amphibole is parallel, but intermediate, to the joins Ed-Tr and Pg-Hbl, indicating that this mineral involves a combination of two reactions that Blundy & Holland (1990) consider occurring between amphibole, quartz and albite in coexisting plagioclase:

(1) edenite + 4 quartz = tremolite + albite

(2) pargasite + 4 quartz = hornblende + albite

Al tends to replace Si in tetrahedral coordination in Ca-amphibole from metabasites of the SF with increasing temperature, whereas Al substitutes for Fe+Mg in the M2 octahedral site to progressively greater extents with increasing pressure, which has been also shown in different studies (e.g., Raase, 1974; Hawthorne, 1983; Gilbert et al., 1981; Robinson et al., 1982). Accordingly, it seems likely that the Al_2O_3 content of Ca-amphibole increases as a function of both P and T (Moody et al., 1983).

Ti is also increasingly accomodated in the Ca-amphibole M2 octahedral site with increasing temperature (Raase, 1974), but this cation should be less favored by increasing pressure because of the relatively larger ionic radius compared with Al (e.g., Ernst & Liu, 1998). FIGURE 6c shows the Ti content of Ca-amphibole from the SF. Ti content in Ca-amphibole ranges from 0.025 to 0.073, which suggests that this metamorphic unit belongs to the greenschist-amphibolite transition facies. According to Ernst & Liu (1998), it seems probable that Ti concentration in Ca-amphibole will track positively with T, but perhaps slightly negatively with P. In the metabasites of the SF that contain a Ti-rich phase such as ilmenite, titanite, or rutile, and are therefore saturated in Ti, which, in addition, carry appropriate, highly aluminous phases such as plagioclase, epidote, or garnet, the isopleths for Al_2O_3 and TiO_2 in Ca-amphibole should display contrasting behavior. Ideally, for the SF metabasites, the P-T conditions of metamorphism should be obtainable, at least approximately, from analysis of Ca-amphibole, if Al and Ti changes with physical conditions are established.

TABLE 5. Representative chemical compositions of associated phases from metabasites of the Silgará Formation at the southwestern Santander Massif.

Lithology	GBM	MS	MS	A	A	MS	MS	GBM	A	MS	GBM	A	A	A	MS	MS
Met. Zone	St-Ky	St-Ky	St-Ky	St-Ky	Grt	St-Ky	St-Ky	St-Ky	Grt	St-Ky	St-Ky	St-Ky	Grt	Grt	St-Ky	Grt
Mineral	Grt	Bt	Bt	Bt	Bt	Pl	Pl	Pl	Pl	Ep	Ep	Fe-Ti ph.	Fe-Ti ph.	Fe-Ti ph.	Chl	Chl
Sample	PCM-514	PCM-356	PCM-480	PCM-497	PCM-531	PCM-356	PCM-480	PCM-514	PCM-531	PCM-480	PCM-514	PCM-497	PCM-531	PCM-531	PCM-497	PCM-531
Analysis	71	153	43	9	27	71	51	19	36	61	39	90	33	95	22	10
Weight %	rim	mat.	core	core	mat.	aug.	core	mat.	rim	core	mat.	inc.	inc.	inc.	mat.	ret.
SiO_2	36,88	37,63	37,45	38,33	36,55	59,16	59,57	56,78	68,39	38,41	37,33	0,07	0,01	0,06	25,89	26,55
TiO_2	0,04	2,19	2,14	1,37	1,56	0,02	0,00	0,02	0,00	0,12	0,11	98,08	49,52	0,03	0,08	0,03
Al_2O_3	20,28	16,55	16,11	16,32	15,85	25,34	26,07	26,55	19,80	24,95	23,16	0,01	0,07	0,01	22,23	20,27
FeO *	23,39	14,99	14,59	13,19	13,09	0,17	0,09	0,13	0,07	0,00	0,00	0,72	43,63	92,37	15,50	17,91
Fe_2O_3*	0,00	0,00	0,00	0,00	0,00	0,00	0,00	0,00	0,00	10,30	11,67	0,00	0,00	0,00	0,00	0,00
MnO	8,72	0,17	0,26	0,22	0,15	0,00	0,00	0,00	0,00	0,11	0,20	0,02	0,17	0,10	0,20	0,13
MgO	2,86	14,40	14,08	16,56	16,22	0,00	0,00	0,00	0,00	0,00	0,00	0,00	0,00	0,03	22,41	21,49
CaO	6,39	0,00	0,00	0,00	0,00	6,99	8,30	8,71	0,26	24,72	23,34	0,00	0,00	0,00	0,00	0,00
Na_2O	0,00	0,11	0,16	0,11	0,10	7,86	7,43	6,54	11,37	0,00	0,00	0,00	0,00	0,00	0,00	0,00
K_2O	0,00	7,90	10,35	10,07	10,28	0,10	0,13	0,10	0,22	0,00	0,00	0,00	0,00	0,00	0,00	0,00
Cr_2O_3	0,00	0,00	0,00	0,00	0,00	0,00	0,00	0,00	0,00	0,00	0,00	0,08	0,22	1,81	0,00	0,00
Total	98,56	93,94	95,14	96,17	93,80	99,84	101,59	98,83	100,11	98,61	95,81	98,98	93,62	94,41	86,31	86,38
Cations per	12 Oxyg.	22 Oxyg.	22 Oxyg.	22 Oxyg.	22 Oxyg.	8 Oxyg.	8 Oxyg.	8 Oxyg.	8 Oxyg.	25 Oxyg.	25 Oxyg.	2 Oxyg.	3 Oxyg.	4 Oxyg.	28 Oxyg.	28 Oxyg.
Si	2,996	5,611	5,609	5,617	5,523	2,654	2,625	2,575	2,985	6,138	6,185	0,001	0,000	0,003	5,244	5,453
Ti	0,002	0,246	0,241	0,151	0,177	0,001	0,000	0,001	0,000	0,014	0,014	0,992	0,999	0,001	0,012	0,005
Al	1,941	2,908	2,843	2,819	2,822	1,335	1,354	1,419	1,019	4,699	4,522	0,000	0,002	0,001	5,307	4,906
Fe 2+	1,588	1,869	1,827	1,616	1,654	0,006	0,003	0,005	0,003	0,000	0,000	0,008	0,978	3,867	2,625	3,076
Fe 3+	0,000	0,000	0,000	0,000	0,000	0,000	0,000	0,000	0,000	1,376	1,617	0,000	0,000	0,000	0,000	0,000
Mn	0,600	0,021	0,033	0,027	0,019	0,000	0,000	0,000	0,000	0,015	0,028	0,000	0,004	0,004	0,034	0,023
Mg	0,346	3,201	3,144	3,618	3,654	0,000	0,000	0,000	0,000	0,000	0,000	0,000	0,000	0,002	6,767	6,580
Ca	0,556	0,000	0,000	0,000	0,000	0,335	0,392	0,423	0,012	4,232	4,143	0,000	0,000	0,000	0,000	0,000
Na	0,000	0,032	0,046	0,031	0,029	0,681	0,635	0,575	0,962	0,000	0,000	0,000	0,000	0,000	0,000	0,000
K	0,000	1,503	1,977	1,882	1,981	0,006	0,007	0,006	0,012	0,000	0,000	0,000	0,000	0,000	0,000	0,000
Cr	0,000	0,000	0,000	0,000	0,000	0,000	0,000	0,000	0,000	0,000	0,000	0,001	0,005	0,072	0,000	0,000
Total	8,029	15,391	15,720	15,761	15,859	5,021	5,019	5,005	4,993	16,474	16,509	1,002	1,988	3,950	19,989	20,043
X_{Fe}	0,82	0,63	0,63	0,69	0,69							1,00	1,00	1,00	0,28	0,32
X_{alm}	0,51															
X_{sps}	0,19															
X_{prp}	0,16															
X_{grs}	0,18															
X_{An}						0,33	0,38	0,42	0,01							
$Fe^{3+}/(Fe^{3+}+Al)$										0,23	0,26					

*Total Fe as FeO for all mineral phases, except for epidote (*Total Fe as Fe_2O_3). $X_{Fe} = Fe/(Mg+Fe^{2+})$. $X_{An} = Ca/(Ca+Na+K)$.

$X_{alm} = Fe^{2+}/(Fe^{2+}+Mn+Mg+Ca)$, $X_{sps} = Mn/(Fe^{2+}+Mn+Mg+Ca)$, $X_{prp} = Mg/(Fe^{2+}Mn+Mg+Ca)$, $X_{grs} = Ca/Fe^{2+}+Mn+Mg+Ca)$.

Abreviations: MS (mafic schits), A (amphibolite), GBM (garnet-bearing metabasite), mat. (Matrix), inc. (Inclusion), aug. (augen), ret. (retrograde phase).

The linear relationship in FIGURE 6d of near unit slope demostrates that the reaction mechanism in Ca-amphibole tetrahedral (and other) sites with increasing temperature involves edenite, tschermak, and Ti-tschermak substitutions as been reported in different studies (e.g., Kawakatsu & Yamaguchi, 1987; Blundy & Holland, 1990; Ernst & Liu, 1998). The overall change in the analized compositions of amphiboles can be represented by the following substitutions:

(3) edenite $(Na+K)_A,Al^{IV} = ?_A,Si$
(4) tschermak $Al^{VI},Al^{IV} = (Mg,Fe^{2+},Mn),Si$
(5) Ti-tschermak $Ti,Al_2^{IV} = (Mg,Fe^{2+},Mn),Si$

In different studies (e.g., Leake, 1965; Raase, 1974; Graham, 1974; Brown, 1977) have been shown that amphibole composition, particularly Al and Na contents, can be used as a pressure indicator. FIGURE 7 illustrates formula proportion diagrams for Ca-amphibole from the metabasites of the SF at the southwestern Santander Massif compared with amphibole from important world-wide occurrences of metabasic rocks as propossed by Laird & Albee (1981). The Sambagawa and Franciscan terrranes belong to the high-pressure facies series, the Abukuma terrane to the low-pressure andalusite-sillimanite facies series, and the Haast River group and Dalradiam terrane to the medium-pressure kyanite-sillimanite facies series.

These diagrams are dependent of data normalization. According to Laird & Albee (1981), the glaucophane substitution $Na_{(B)},(Al^{VI}+Fe^{3+}+Ti+Cr) = Ca,(Fe^{2+}+Mg+Mn)$ in amphibole dominates during high-pressure facies series metamorphism, while the edenite (3) and tschermak (4) susbtitutions dominate during low-pressure facies series metamorphism. As shown in FIGURE 7a, chemical compositions of amphibole above the line actinolite-tschermakite require glaucophane substitution to maintain charge balance and those below this line show edenite substitution. Amphibole analyses from the metabasites of SF are plotted between high- and low-pressure facies series. FIGURE 7b shows that the amphibole analyses from the metabasites considered in this study are plotted mainly in the Abukuma terrane and the Haast River group, although they are overlaping into the Sambagawa & Franciscan and Dalradiam terranes, particularly at low $Na_{(B)}$ contents. From this diagram can be established that increasing pressure generally reflects an increase in amphibole of the parameter plotted along the vertical axis, and increasing temperature generally reflects an increase in the parameter plotted along the horizontal axis. $Na_{(B)}$ in amphibole tends to increase with increasing $Al^{VI}+Fe^{3+}+Ti$, and should increase with increasing metamorphic grade (presure and temperature conditions).

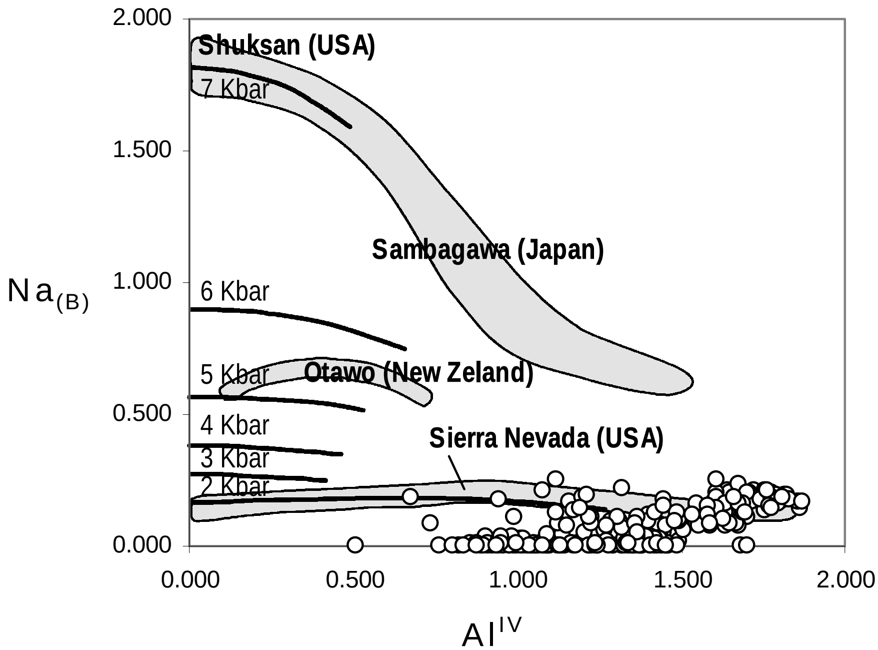

FIGURE 5. Chemical compositions of Ca-amphibole from metabasites of the Silgará Formation (indicated by white dots) in terms of Na(B) vs AlIV, after Brown (1977), showing the typical pressure conditions of important geological frameworks such as Shuksan and Sierra Nevada in USA, Sambagawa in Japan, and Otawo in New Zeland.

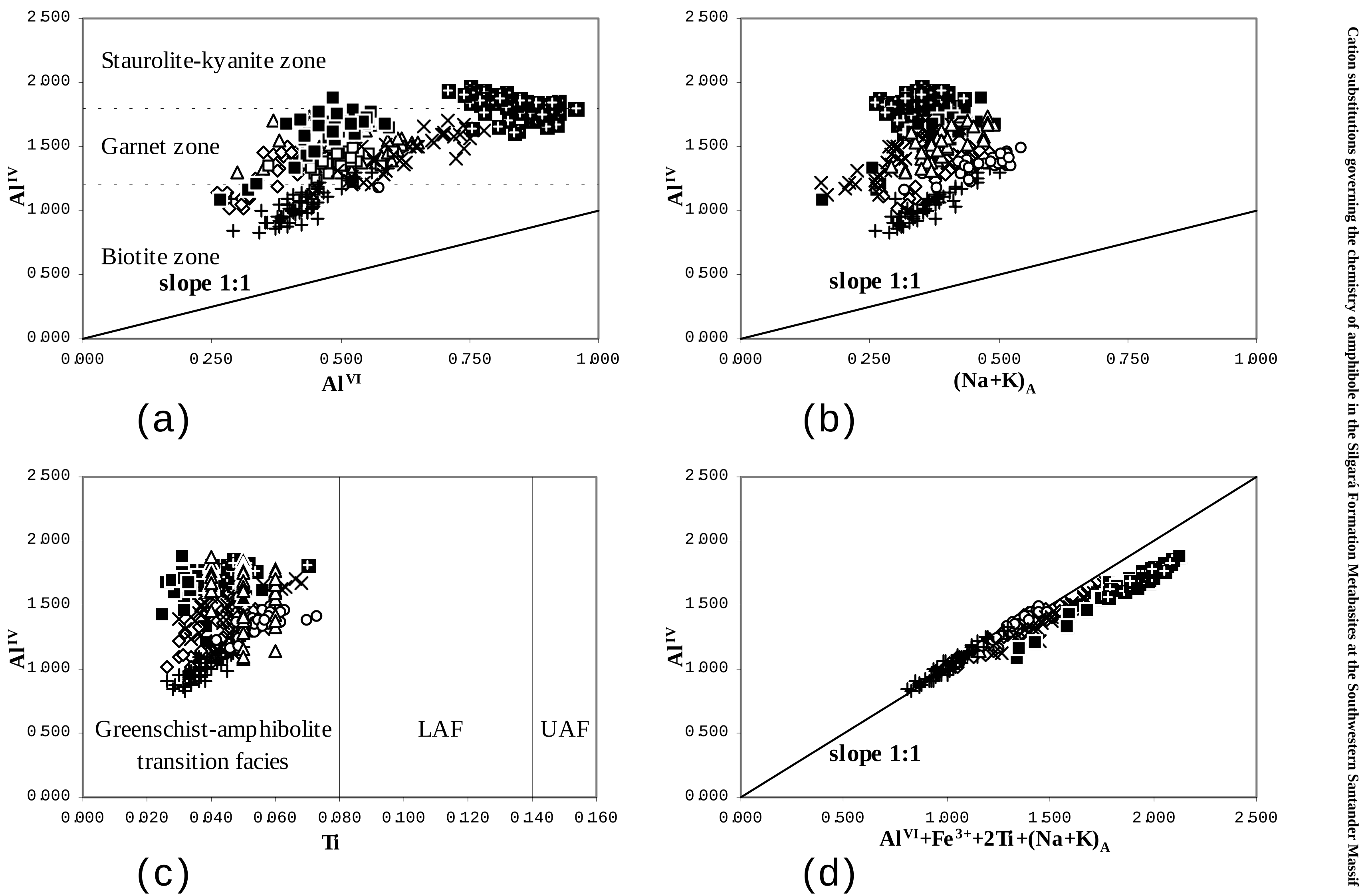

FIGURE 6. Chemical compositions of Ca-amphibole from metabasites in terms of Al on the T1site (Al^{IV}) vs (a) Al on the M2 site (Al^{VI}), after Laird & Albee (1981), (b) A-site occupancy, after Blundy & Holland (1990), (c) Ti on the M2 site, after Rasse (1974), LAF, Lower Amphibolite Facies, and UAF, Upper Amphibolite Facies, and (d) $Al^{VI}+Fe^{3+}+2Ti+(Na+K)_A$, after Kawakatsu & Yamaguchi (1987).

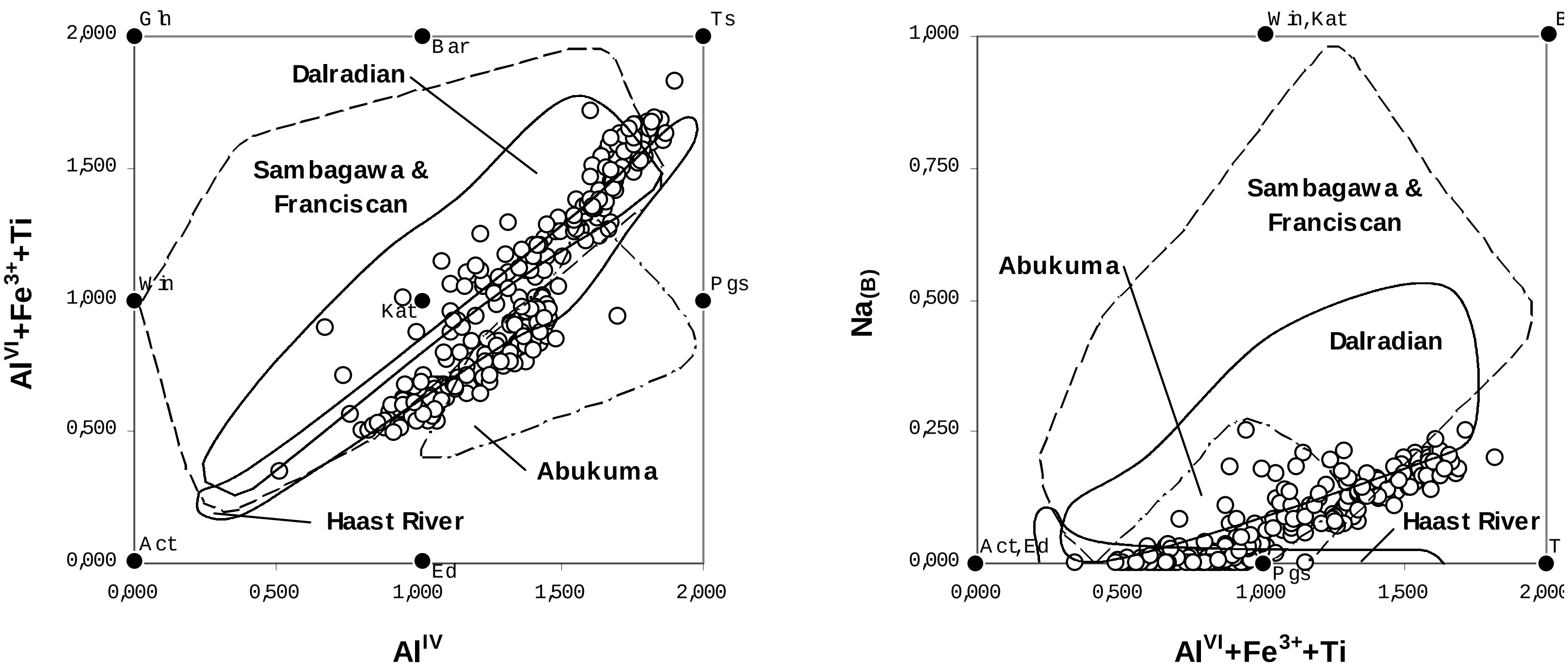

FIGURE 7. Formula proportion diagrams, expressed as (a) $Al^{VI}+Fe^{3+}+Ti$ vs Al^{IV} and (b) $Na_{(B)}$ vs $Al^{VI}+Fe^{3+}+Ti$, for Ca-amphibole from metabasites of the Silgará Formation at southwestern Santander Massif compared with amphibole from important world-wide occurrences of metabasic rocks (after Laird and Albee, 1981), including the high-pressure facies series Sambagawa (Japan) and Franciscan (California) terranes, the medium-pressure Dalradian terrane in southwestern Scotland and Haast River Schist group in New Zealand, and the low-pressure Abukuma terrane in Japan. Endmember amphibole compositions are indicated as black dots: Act (actinolite), Bar (barroisite), Ed (edenite), Gln (glaucophane), Kat (katophirite), Pgs (pargasite), Ts (tschermakite), and Win (winchite). Ca-amphibole compositions of the Silgará Formation are indicated by open circles.

CONCLUDING REMARKS

The aim of the present investigation was a detailed study of all constituents of metabasites of the SF to get a full insight in the metamorphic paragenesis. However, there is no doubt that the rock composition is clearly dominant and obscures the systematic compositional changes caused by pressure and temperature, and therefore bulk-rock chemistry has a strong influence on chemistry of constituent minerals such as amphibole.

The mineral assemblages in metabasites indicate that these rocks have been equilibrated under metamorphic conditions from the greenschist facies to the lower amphibolite facies.

Changes in the chemical composition of Ca-amphibole are interpreted through coupled substitutions, and reactions with co-existing minerals during an increase in metamorphic conditions from greenschist to lower amphibolite facies.

Plagioclase systematically changes its composition in the greenschist-amphibolite facies, and the transition from albite to oligoclase or andesine occurs discontinuously with no plagioclase of composition An_{5-20} (Maruyama *et al.*, 1983), as been reported in this study (An_{5-14}), showing an asymmetrical solvus in the range of peristerite plagioclase, which is suggested to explain this discontinuity and to define the transition between the greenschist facies and the lower amphibolite facies. The Silgará Formation reached the lower amphibolite facies as the peak of metamorphism and then was affected by a retrograde metamorphism may be into the epidote-amphibolite facies. Retrogressive effects are stronger in rocks near to the contact with the Pescadero intrusive.

These results are consistent with those found in pelitic rocks, in which mineral zones (biotite-, garnet-, and staurolite-zones) developed defining the regional thermal structure of the Silgará Formation.

There is not doubt that the bulk-rock chemistry is dominant and obscures the systematic compositional changes caused by pressure and temperature.

ACKNOWLEDGEMENTS

The author is greatlty indebted to Japan - Inter-American Development Bank Scholarship Program through grant to carry out a MSc study at Shimane University. The research was supported by grants from Shimane University and Research Center for Coastal Laggon Environments, and I am indebted to these institutions for allowing me the use of the electron microprobe analyzer. Universidad Industrial de Santander and COLCIENCIAS through Grant No. 1102-05-083-95 financially supported fieldwork. Thanks to my supervisor, Professor Dr. Sc. Akira Takasu, who helped both with useful comments and discussion and assistance with the electron microprobe data acquisition. Special thanks to doctors B. Rosser, A. Tsunagae and M. Akasaka for numerous discussions and constructive comments. The author is most grateful to the above-named people and institutions for support.

REFERENCES

Anderson, J., and Smith, D. (1995). The effects of temperature and fO_2 on the Al-in-hornblende barometer. American Mineralogist, Vol. 80, pp. 549-559.

Bence, A., and Albee, A. (1968). Empirical correction factors for the electron microanalysis of silicates and oxides. Journal of Geology, Vol. 76, pp. 382-403.

Blundy, J., and Holland, T. (1990). Calcic Ca-amphibole equilibria and a new Ca-amphibole plagioclase geothermometer. Contributions to Mineralogy and Petrology, Vol. 104, pp. 208-224.

Brown, E. (1977). The crossite content of Ca-amphibole as a guide to pressure of metamorphism. Journal of Petrology, Vol. 18, pp. 53-72.

Castellanos, O. (1999). Estudio mineralógico y petrográfico de la Formación Silgará en la Franja Pescadero-Aratoca (Santander). Tesis de Pregrado, Universidad Industrial de Santander, Bucaramanga (Colombia).

Deer, W.A., Howie, R.A., and Zussman, J. (1983) Rock-forming Minerals, Chain Silicates, Vol. 2, Wiley, New York, 379p.

Dörr, W., Grösser, J., Rodriguez, G., and Kramm, U. (1995). Zircon U-Pb age of the Paramo Rico tonalite-granodiorite, Santander Massif (Cordillera Oriental, Colombia) and its geotectonic significance. Journal of South American Earth Sciences, Vol. 8(2), pp.187-194.

Ernst, W., and Liu, J. (1998). Experimental phase study of Al- and Ti-contents of calcic Ca-amphibole in MORB – A semiquantitative thermobarometer. American Mineralogist, Vol. 83, pp. 952-969.

Forero, A. (1990). The basement of the Eastern Cordillera, Colombia: An allochthonous terrane in northwestern South America. Journal of South American Earth Sciences, Vol. 3(23), pp. 141-151.

García, C., y Castellanos O. (1998). Petrografía de la Formación Silgará en la Cordillera Oriental, Colombia. X Congreso Latinoamericano de Geología, Buenos Aires, Argentina, Memorias, Vol. 2, pp. 263-268.

García, C., y Ríos, C. (1999). Metamorfismo y metalogenia asociada del Macizo de Santander, Cordillera Oriental, Colombia. Informe final Proyecto de Investigación. Universidad Industrial de Santander-Colciencias, 191p.

Gélvez, J., y Márquez, R. (2002). Caracterización textural del granate y de sus elementos de deformación asociados, y modelamiento de su historia de nucleación y crecimiento en las rocas metapelíticas de la Formación Silgará en la región suroccidental del Macizo de Santander. Tesis de Pregrado, Universidad Industrial de Santander, Bucaramanga (Colombia).

Gilbert, M., Helz, R., Popp, R., and Spear, F. (1981). Experimental studies of amphibole stability. Rev. Mineral., Vol. 9B, pp. 229-353.

Goldsmith, R., Marvin, R., and Mehnert, H. (1971). Radiometric ages in the Santander Massif, eastern Cordillera, Colombian Andes. U.S. Geol. Survey Prof. Paper, Vol. 750-D, pp. D41-D49.

Graham, C. (1974). Metabasite amphiboles of the Scottish Dalradian. Contributions to Mineralogy and Petrology, Vol. 47, pp. 165-185.

Graham, C., and Powell, R. (1984). A garnet-hornblende geothermometer: calibration, testing and application to the Pelona Schist, Southern California. Journal of Metamorphic Geology, Vol. 2, pp. 13-131.

Hammarstrom, J., and Zen, E. (1992). Discussion of Blundy and Holland's (1990) "Calcic Ca-amphibole equilibria and a new amphibole-plagioclase geothermometer". Contributions to Mineralogy and Petrology, Vol. 111, pp. 264-266.

Hawthorne, F. (1983). Crystal chemistry of the amphiboles. Canadian Mineralogist, Vol. 21, pp. 174-481.
Hey, M. (1954). A new review of the chlorites. Mineralogical Magazine, Vol. 25, pp. 277-292.

Holland, T., and Blundy, J. (1994). Non-ideal interactions in calcic amphiboles and their bearing on amphibole-plagioclase thermometry. Contributions to Mineralogy and Petrology, Vol. 116, pp. 433-447.

Johnson, M., and Rutherford, M. (1989). Experimental calibration of the aluminum-in-hornblende gebarometer with application to Long Valley Caldera (California) volcanic rocks. Geology, Vol. 17, pp. 837-841.

Kawakatsu, K., and Yamaguchi, Y. (1987). Successive zoning of amphiboles during progressive oxidation in the Daito-Yakota granitic complex, San-in belt, southwest Japan. Geochimica et Cosmochimica Acta, Vol. 51, pp. 535-540.

Kohn, M., and Spear, F. (1989). Empirical calibration of geobarometers for the assemblage garnet+hornblende+plagioclase+quartz. American Mineralogist, Vol. 74, pp. 77-84.

Kretz, R. (1983). Symbols for rock-forming minerals. American Mineralogist, Vol. 68, pp. 277-279.

Laird, J., and Albee, A. (1981). Pressure, temperature, and time indicators in mafic schist: their application to reconstructing the polymetamorphic history of Vermont. American Journal of Science, Vol. 281, pp. 127-175.

Leake, B. (1965). The relationship between tetrahedral aluminium and the maximum possible octahedral aluminium in natural calciferous and sub-calciferous amphiboles. American Mineralogist, Vol. 50, pp. 843-851.

Leake, B., Woolley, A., Arps, C., Birch, W., Gilbert, M., Grice, J., Hawthorne, F., Kato, A., Kisch, H., Krivovichev, V., Linthout, K., Laird, J., Mandarino, J., Maresch, W., Nickel, E., Rock, N., Schumacher, J., Smith, D., Stephenson, N., Un-garetti, L., Whittaker, E., and Youzhi, G. (1997) Nomenclature of amphiboles: Report of the Subcommittee on Amphiboles of the International Mineralogical Association, Commission on New Minerals and Mineral Names. American Mineralogist, Vol. 82, pp. 1019– 1037.

Mantilla, L., Ordoñez, J., Cepeda, S., and Ríos, C. (2001). Study of the paleofluids in the Silgará Formation and their relationship with deformation processes, Aratoca-Pescadero area (southwestern Santander Massif). Boletín de Geología UIS, Vol. 23 (38), pp. 69-75.

Mantilla, L., Ríos, C., and Castellanos, O. (2002). Study of the rehydratation process of the Silgará Formation metamorphic rocks, from the compositional analysis of chlorite, southwestern Santander Massif. Boletín de Geología UIS, Vol. 24 (39), pp. 7-17.

Mantilla, L., Ríos, C., Gélvez, J., Márquez, R., Ordoñez, J., and Cepeda, S. (2003). New evidences on the presence of a shear band in the metapelitic sequence of the Silgará Formation, Aratoca-Pescadero area (southwestern Santander Massif). Boletín de Geología UIS, Vol. 25 (40), pp. 81-89.

Maruyama, S., Suzuki, K., and Liou, J. (1983). Greenschist-amphibolite transition equilibria at low pressures. Journal of Petroloy, Vol. 24, pp. 585-604.

Moody, J., Meyer, D., and Jenkins, J. (1983). Experimental characterization of the greenschist/amphibolite boundary in mafic systems. American Journal of Science, Vol. 283, pp. 48-92.

Neogi, S., Dasgupta, S., and Fukuoka, M. (1997). High P-T polymetamorphism, dehydration melting, and generation of migmatites and granites in the Higher Himalayan Crystalline Complex, Sikkim, India. Journal of Petrology, Vol. 39, pp. 61-99.

Ordoñez, J. (2003). Petrology and geochemistry of the granitoids at the Santander Massif, Eastern Cordillera, Colombian Andes. MSc Tesis, Shimane University, Matsue (Japan), 207p.

Poli, S., and Schmidt, M. (1992). “Calcic Ca-amphibole equilibria and a new amphibole-plagioclase geothermometer” by J. Blundy and T. Holland (Contributions to Mineralogy and Petrology (1990) 104: 208-224). Contributions to Mineralogy and Petrology, Vol. 111, pp. 273-278.

Raase, P. (1974). Al and Ti contents of hornblende, indicators of pressure and temperature of regional metamorphism. Contributions to Mineralogy and Petrology, Vol. 45, pp. 231-236.

Ríos, C. (1999). Chemical Compositions of the Constituent Minerals and P-T Conditions of the Low-grade Silgará Formation Metamorfic Rocks in the Santander Massif, Eastern Cordillera, Colombian Andes. MSc Tesis, Shimane University, Matsue (Japan), 207p.

Ríos, C., and Takasu, A. (1999). Chemical zoning of garnet from the low-grade metamorphic rocks of the Silgará Formation, Santander Massif, Eastern Cordillera (Colombian Andes). Geosciences Reports of Shimane University, Vol. 18, pp. 97-107.

Ríos, C. (2001). Occurrence, chemical composition and genetic significance of the biotite in the Silgará Formation metamorphic rocks, southwestern Santander Massif, Eastern Cordillera, Colombian Andes. Boletín de Geología UIS, Vol. 23 (38), pp. 41-49.

Ríos, C., and García, C. (2001). First occurrence of the three Al_2SiO_5 polymorphs in the Silgará Formation metapelitic rocks, southwestern Santander Massif, Eastern Cordillera, Colombian Andes. Boletín de Geología UIS, Vol. 23 (38), pp. 51-59.

Ríos, C., García, C., and Takasu, A. (2003). Tectono-metamorphic evolution of the Silgará Formation metamorphic rocks in the southwestern Santander Massif, Colombian Andes. Journal of South American Earth Sciences, Vol. 16, pp. 133-154.

Robinson. P., Spear, F., Schumacher, J., Laird, J., Klein, C., Evans, B., and Doolan, B. (1982). Phase relations of metamorphic amphiboles: natural occurrence and theory. In: Veblen, D.R., Ribbe, P.H. (Eds.), Amphiboles: Petrology and Experimental Phase Relations. Rev. Mineral., Vol. 9B, pp, 1-227.

Rutherford M., and Johnson, M. (1992). Comment on Blundy and Holland‘s (1990) “Calcic Ca-amphibole equilibria and a new amphibole-plagioclase geothermometer”. Contributions to Mineralogy and Petrology, Vol. 111, pp. 266-268.

Schäfer, J., Grösser, J., and Rodríguez, G. (1998). ?Proterozoic Formation Silgará, Cordillera Oriental, Colombia: metamorphism and geochemistry of amphibolites. Zbl. Geol. Paläont. Teil I, 1997 (3-6), Stuttgart, pp. 531-546.

Spear, F. (1980). NaSi=CaAl exchange equilibrium between plagioclase and amphibole: an empirical model. Contributions to Mineralogy and Petrology, Vol. 72, pp. 33-41.

Thompson, J., Laird, J., and Thompson, A. (1982). Reactions in amphibolite, gereenschist and blueschist. Journal of Petrology, Vol. 23, pp. 1-27.

Ward, D., Goldsmith, R., Cruz, B., Jaramillo, C., and Restrepo, H. (1973). Geología de los Cuadrángulos H-12, Bucaramanga y H-13, Pamplona, Departamento de Santander. U.S. Geological Survey e Ingeominas. Boletín Geológico, Vol. XXI(1-3), 132p.

Trabajo recibido: octubre 5 de 2004
Trabajo aceptado: febrero 1 de 2005